Analyst

PAPER

View Article Online
View Journal | View Issue

Cite this: *Analyst*, 2014, **139**, 778

Mediatorless N_2 incorporated diamond nanowire electrode for selective detection of NADH at stable low oxidation potential

Jayakumar Shalini,[a] Kamatchi Jothiramalingam Sankaran,[a] Huang-Chin Chen,[b] Chi-Young Lee,*[a] Nyan-Hwa Tai[a] and I-Nan Lin*[b]

The electrocatalytic properties of a N_2 incorporated diamond nanowire (N-DNW) unmodified electrode towards the oxidation of nicotinamide adenine dinucleotide (NADH) was critically evaluated. The electrochemical behavior of the N-DNW unmodified electrode was examined and compared with that of boron-doped diamond, glassy carbon electrode, and graphite electrodes. The N-DNW electrode had high selectivity and high sensitivity for the differential pulse voltammetric detection of NADH in the presence of ascorbic acid at the lower and stable oxidation potential. Moreover, it exhibited strong stability after prolonged usage. The oxidation peak potential at the N-DNW electrode remained unchanged even after exposure to the solution, followed by washing, drying, and storage in laboratory air for 20 days, with minimization of surface contamination. Therefore, the N-DNW unmodified electrode shows promise for the detection of NADH and is attractive for use in a dehydrogenase based biosensor and other analytical applications.

Received 27th June 2013
Accepted 8th November 2013

DOI: 10.1039/c3an01246h

www.rsc.org/analyst

1. Introduction

The electrochemical (EC) oxidation of nicotinamide adenine dinucleotide (NADH) is of great interest because NAD/NADH is a crucial coenzyme couple. It plays a vital role in various enzymatic reactions of NADH-dependent dehydrogenases which catalyze the oxidation of ethanol or lactic acid.[1–9] However, the direct EC oxidation of NADH to NAD^+ at bare electrode surfaces is highly irreversible and takes place at high (*ca.* >+0.5 V) overpotentials.[10–14] This required high overpotential also oxidizes other electroactive species that may be present in the solution being analysed.[3] The oxidized NADH produces NAD^+, which forms dimers and other oxidation products such as, methyl, propyl and benzyl reactants. These products can be strongly adsorbed on the electrode surface[15–18] which hinders the heterogeneous charge transfer and causes deactivation of the electrode. Thus, leading to surface fouling of the electrode[14] which ultimately produces a system lacking in sensitivity.[19–23]

In most cases, the high overpotential required for NADH electrooxidation has been reduced through the use of redox mediators. Different electron mediators such as water soluble dye compounds[24,25] phenothiazine derivatives[26] phenyl azo aniline[27] adenine derivatives[28] and various redox polymers[29] have been employed to allow for efficient electron transfer, reduction of overpotential, and prevention of surface fouling of the electrode. However promising the use of such mediators seems, they still cause problems such as leakages from the electrode surface, lack of long-term stability and toxicity, thereby limiting their analytical applications.[30] Recently, much effort has been devoted to developing new nanomaterials, in particular carbon nanotubes (CNTs), to reduce the overpotential required for NADH oxidation and to minimize the surface contamination effect without the use of any redox mediators. Nanomaterials have attractive EC properties (stability and sensitivity),[31,32] because of their good biocompatibility, low toxicity, large surface area and easy preparation processes .[33,34] The biocompatibility and EC applications of CNTs for the immobilization of a variety of species have been reported.[26,30,35] Pyrolytic graphite electrodes have been used to study the EC oxidation of NADH and carbon electrodes by Moiroux and Elving,[19,21,22,36] to elucidate the mechanism of oxidation but not for analytical purposes. Furthermore, literature reports[22,36] imply that the electron transfer is more facile in samples containing a higher proportion of edge plane defects than for basal plane graphite electrodes.

In recent years, biosensors based on diamond have attracted immense attention as diamond is known to be biocompatible and chemically inert, it has excellent EC properties and biomolecules bonded to it have long-term chemical stability. Precisely, diamond electrodes prepared by chemical vapor deposition processes possesses enhanced EC properties for a wide range of applications.[37–39] These diamond electrodes synthesized by using either a nitrogen or boron source possess

[a]*Department of Material Science and Engineering, National Tsing Hua University, Hsinchu 300, Taiwan, People's Republic of China. E-mail: cylee@mx.nthu.edu.tw*
[b]*Department of Physics, Tamkang University, New Taipei 251, Taiwan, People's Republic of China*

high surface to volume ratios with significant π-bonding and sp^2 hybridization[40–42] resulting in high electrical conducting behavior with distinct EC properties.[43,44] Particularly, boron-doped diamond (BDD) electrodes have been widely employed for the construction of various EC biosensors due to their remarkable properties, including a wide EC potential window in aqueous and non-aqueous media, low and stable capacitive background current, high response reproducibility and good biocompatibility.[45–48] Conductive diamond is an excellent material owing to its high mechanical strength. Recently, an ethanol biosensor based on the determination of NADH generated in the enzymatic reaction catalyzed by alcohol dehydrogenase was examined in order to demonstrate the use of unmodified highly doped BDD electrodes in biosensors. For instance, the research group of Fujishima described the EC detection of NADH in the presence of AA at highly doped BDD electrodes.[49–51] Despite these significant developments, the voltammetric current response for BDD electrodes was observed at +0.58 V. Such a high overpotential will also oxidize other electroactive species that may be present in the solution being analyzed. The peak corresponding to the AA oxidation appears as a shoulder in the voltammogram for the mixture of AA and NADH solution and thus the selectivity is still not sufficiently satisfactory. It would be highly noteworthy to look for efficient as well as convenient unmodified new electrode materials for the simultaneous detection of NADH with stable low oxidation potential along with good selectivity.

Introduction of N_2 gas in the growth plasma results in extreme modification of the properties of diamond materials. Incorporation of N_2 in the growth plasma leads to an increase in an amorphous carbon phase which in turn converts to a graphitic phase on annealing. Defects contributing to the sp^2 at the grain boundaries, leads to an increase in the overall grain boundary volume with an increase in the density of states at the Fermi level.[52–54] Studies of the effect of changes in the morphology of the electrodes with changes in different electrode deposition parameters on the properties of the structural properties and electrical conductivity have been carried out.[55–63] On the other hand, N_2 incorporated diamond nanowire (N-DNW) films have hardly been demonstrated as EC electrodes for the detection of NADH without electrode surface modification. To the best of our knowledge the simultaneous detection of NADH and AA based on N_2-incorporated diamond electrodes has not been reported yet. Herein, we report for the first time on the simultaneous detection of NADH and AA using an N-DNW unmodified electrode without any surface modification (addition of electron transfer mediator or specific reagents) by differential pulse voltammetry (DPV).

2. Experimental

2.1. Chemicals and reagents

NADH and ascorbic acid of reagent grade quality were purchased from Aldrich chemicals and were used without further purification. All the solutions containing redox-active solutes were freshly prepared. Phosphate buffer solution (PBS, pH 7.4) was prepared from sodium dihydrogen phosphate and disodium hydrogen phosphate and was used as the supporting electrolyte throughout the EC studies. BDD was purchased from Kinik Company, Taiwan and was used without any further pretreatment.

2.2. Analytical method

The EC properties of the N-DNW and bare electrodes were characterized using cyclic voltammetry (CV, Autolab PGSTAT302, Netherlands). These measurements were carried out using a CS-1087 computer-controlled potentiostat (CV Autolab PGSTAT302, Netherlands). A standard three electrode cell was employed. N-DNW film was used as the working electrode (working area of 0.186 cm^2). A platinum (Pt) rod and silver/silver chloride (Ag/AgCl) electrodes served as the counter and reference electrodes respectively. All the potentials in this study were reported with respect to an Ag/AgCl electrode. All the measurements were carried out at room temperature in 0.1 M PBS solution of pH 7.4. De-ionized water was used throughout the experiments.

2.3. Preparation of the N-DNW electrode

N-DNW films were grown on planar Si substrates using the microwave plasma enhanced chemical vapor deposition (MPECVD) method. Prior to the deposition, the substrates were ultrasonicated in methanol solution, containing nano-diamond powder (~5.0 nm) and titanium powder (~37.0 μm), for 45 minutes to create nucleation sites. The nitrogen and methane gas flow was controlled at 94% sccm and 6% sccm with a mass flow controller respectively. The total pressure in the reactor was 120 Torr, and the substrate temperature (T_s) was estimated to be 700 °C. The deposition of the film was carried out at a microwave power of 1200 W. A film thickness of ~500 nm was achieved after 30 minutes of deposition. The morphology and microstructure of the N-DNW film were examined using field emission scanning electron microscopy (FESEM; JEOL-6500F) and transmission electron microscopy (TEM; JEOL-2100 operated at 200 kV). The bonding character of different types of carbon in the N-DNW films was characterized by visible-Raman spectroscopy (λ: 632.8 nm, Lab Raman HR800, Jobin Yvon).

3. Results and discussion

3.1. Microstructural characterization

Fig. 1a shows an FESEM image of the densely packed N-DNW films grown at $T_s = 700$ °C in the MPECVD system possessing a characteristic 'acicular' like structure with a width of a few nanometers. The inset of Fig. 1a depicts the Raman spectrum, characterized by broad peaks at ~1367 cm^{-1} (D-band), arising from optical phonons of the disordered sp^2-bonded carbon atoms, and ~1511 cm^{-1} (G-band), indicative of scattering due to the ordered sp^2-bonded carbon at the grain boundaries in the films.[64–70] A small peak at ~1162 cm^{-1} corresponds to the *trans*-polyacetylene (*t*-PA) domains.[71–75] The broad peaks are suggestive of phonon scattering and intrinsic stress due to nanosized grains of defective diamond.[76]

Fig. 1b shows a typical low-magnification TEM image of an N-DNW film, revealing the highly dense and uniformly distributed nanowire morphology. These randomly oriented

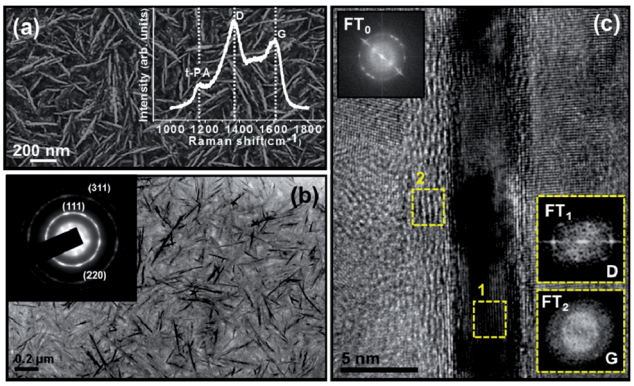

Fig. 1 (a) FESEM image of N-DNW films. The inset shows the visible-Raman spectrum of the N-DNWs films. The characteristic peaks of *trans*-polyacetylene, diamond, and graphite bands are marked as *t*-PA, D, and G, respectively. (b) Bright field TEM image of N-DNW films. The inset shows the SAED pattern of the corresponding TEM image, where lattice-plane spacings of the diamond are indicated. (c) HRTEM image with its corresponding FT (FT_0) pattern displayed in the inset. FT patterns of areas '1' and '2' in TEM image (c) are shown in figures FT_1 and FT_2, respectively.

N-DNW films have a length of 50–200 nm with a diameter of a few nanometers. The selective area electron diffraction (SAED) pattern of the corresponding TEM image of the N-DNW film is shown in the inset of Fig. 1b, it exhibits ring-shaped patterns, implying random orientation of the N-DNWs that are observed in the TEM image (Fig. 1b). According to the SAED pattern, the lattice-plane spacings of (311), (220), and (111) are estimated to be 0.11, 0.12, and 0.21 nm, respectively, which are in line with the crystalline diamond structure. The results confirm that N-DNW films, rmainly consist of diamond nanocrystals with nanowire morphology. On the other hand, there is a prominent diffusing ring in the center of the SAED pattern, signifying the existence of a graphitic phase in the N-DNW film. To analyze the two crystalline carbon phases of the diamond and graphite structures in detail an HRTEM image (Fig. 1c) was taken and its corresponding Fourier Transform (FT) pattern is displayed in the inset (FT_0). Selected areas of the diamond and graphitic structures were further analyzed by FT. FT_1 (inset of Fig. 1c) shows the FT pattern of area '1' (marked in Fig. 1c) giving the ordering of the (111) planes of the diamond structure whereas FT_2 (inset of Fig. 1c) shows the FT pattern of area '2' pointing to the ordering of the (111) planes of the graphitic structure. These results are evidence that the N-DNWs are encapsulated by a sheath of graphitic phase. The microstructural studies of the N-DNW films confirmed that this graphitic content is formed during the growth of films.[63,77]

Moreover, CVs based on ferricyanide redox reactions performed at various scan rates are often used to estimate the active surface areas (ASA) of electrodes by using the Randles–Sevcik equation ($I_p = 2.69 \times 10^5\, AD_o^{1/2} n^{3/2} C_o \upsilon^{1/2}$).[78] Here, I_p is the reduction peak current in mA, A is the electrode ASA in cm^2, D_o is the diffusion coefficient of ferricyanide (7.01×10^{-6} cm^2 s^{-1}),[79] n is the number of electrons transferred in the reaction equation, C_o is the concentration of ferricyanide in M, and υ is the scan rate in V s^{-1}. The calculated active surface areas of the N-DNW and BDD electrodes were 0.254 cm^2 and 0.202 cm^2. These observations clearly confirm the formation of a DNW-like film structure which can be employed for EC electrode applications due to its larger surface area and low charge transfer resistance, and opens the possibility of an entire series of biosensor applications.

3.2. Electrocatalytic oxidation of NADH on the N-DNW film electrode

Bare electrodes very often suffer from fouling by the adsorption of oxidation products. Thus, the direct oxidation of NADH at unmodified electrodes is not straightforward and requires high overpotential (usually 0.7–1.0 V) owing to the sluggish electron-transfer kinetics.[80] Various methodologies have been developed to enhance the electron-transfer kinetics of the oxidation of NADH.[81] Recently, much effort has been devoted to developing new nanomaterials which can effectively overcome the kinetic barriers for the oxidation of NADH and regenerate the enzymatically active NAD^+.[82] Carbon nanotubes (CNTs) have received considerable attention for this purpose. Many studies have demonstrated that CNTs can be used to fabricate nanostructured macroscopic electrodes, biosensors, and nanobioelectronic devices due to their nanometer size, lack of toxicity, good electrocatalytic properties, efficient accumulation of biomolecules as well as minimization of surface fouling.[83] Although CNTs-based electrodes are known to decrease the overpotential for the oxidation of NADH, the extent of decrease is not sufficient enough for the selective detection of NADH.[84] The oxidation of NADH at potentials of more than 0.34 V (*vs.* NHE) often suffers from much interference. Therefore, it is essential to develop an electrode, which can catalyze the oxidation of NADH at a lower positive potential. Fig. 2 depicts a typical comparison of CV responses from the EC oxidation of 0.1 mM NADH at N-DNW and BDD electrodes in PBS (pH 7.4). A shift in the peak current at the N-DNW electrode was observed due to the large electrochemically active surface area (0.254 cm^2) and fast electron transfer reaction.[78,79] Additionally, due to the EC stability of the corresponding redox couple at the N-DNW unmodified electrode, it can be used as a mediatorless EC system to shuttle electrons between the N-DNW electrode and NADH. As can be seen, a

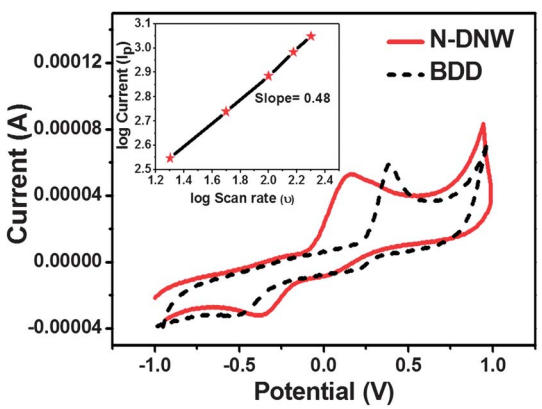

Fig. 2 Cyclic voltammogram of N-DNW and BDD electrodes in 0.1 mM PBS (pH 7.4) at a scan rate of 50 mV s^{-1}. Inset: log current (I_p) *versus* log scan rate (υ) plot for the N-DNW electrode.

similar voltammetric response was observed for both the N-DNW and BDD electrodes at the EC oxidation. The anodic oxidation of NADH takes place at a relatively lower potential of +0.15 V on a N-DNW electrode, whereas the BDD exhibits a significant shift in the high peak potential to +0.45 V. It is obvious that the presence of N-DNW leads to enhanced peak currents and lower oxidation potentials. Moreover, the oxidation peak potential of +0.15 V for the N-DNW electrode is lower than that of the BDD electrode (+0.3 V). This is probably due to the incorporation of nitrogen in diamond films which can cause defects and the creation of sp^2 carbon in the grain boundaries.[63] Therefore, it has been suggested that many dangling bonds present in the grain boundaries of N-DNW film electrodes are responsible for the enhanced EC sensing. Diamond films have been reported to have high resistance to electrode fouling[1] because the lack of polar oxygen-containing functional groups on the surface of the N-DNW electrode is responsible for the lack of adsorption and resistance to electrode fouling by NAD^+.[1,85] Furthermore, the results obtained with for the N-DNW electrode are in agreement with literature reports whereas GC electrodes are highly susceptible to electrode passivation by the strong adsorption of the NAD^+ produced from the oxidation of NADH.[1,2,23]

To observe the kinetic characteristics of NADH oxidation, CV of the N-DNW electrode was investigated at variable scan rates. The anodic peak current and the peak potential were shifted towards the positive direction with an increase in the scan rate. An excellent linearity was observed for the peak current (I_p) *versus* the square root of the potential scan rate ($v^{1/2}$) which endorses the EC irreversibility of the electrocatalytic reaction. A slope of ~0.48 from the $\log(I_p)$ *versus* $\log(v)$ plot (inset of Fig. 2) suggests that the oxidation of NADH is diffusion controlled from the solution to the redox sites at the N-DNW electrode. The mechanism of the EC NADH oxidation in the N-DNW system can be depicted as follows:

$$\mathrm{DNW/NADH} - \mathrm{e}^- \xrightarrow{\text{adsorption}} \mathrm{DNW/NADH}^{\cdot+} \quad (1)$$

$$\mathrm{DNW/NADH}^{\cdot+} \xrightarrow{-\mathrm{H}^+} \mathrm{DNW/NAD}^{\cdot} \quad (2)$$

$$\mathrm{DNW/NAD}^{\cdot} - \mathrm{e}^- \xrightarrow{\text{desorption}} \mathrm{DNW/NAD}^+ \quad (3)$$

overall reaction

$$\mathrm{DNW/NADH} \rightarrow \mathrm{DNW/NAD}^+ + 2\mathrm{e}^- + \mathrm{H}^+ \quad (4)$$

where NADH diffuses and adsorbs on the electrode surface and then is electrochemically oxidized by an ECE (Electron transfer – Chemical reaction – Electron transfer) mechanism.[22] According to the ECE mechanism, the first step of NADH electrochemical oxidation is an irreversible heterogeneous electron transfer. In this step, one electron is lost and a cation radical $NADH^{\cdot+}$ is produced in eqn (1). The neutral radical $NAD^{\cdot}$ was produced through a first-order de-protonation reaction of $NADH^{\cdot+}$ in eqn (2). A continual reaction for electron transfer from $NAD^{\cdot}$ occurred through a second heterogeneous electron transfer in eqn (3). In this system, the N-DNW electrode plays the role of an electrocatalyst for NADH oxidation while the sp^2 graphitic phase encasing the nanowire-like structure of the diamond film works as an electron carrier. Overall the electro-oxidation of NADH at N-DNW involves two separate electron transfer processes eqn (4).

3.3. Interference by ascorbic acid

To evaluate the possibility of the simultaneous detection of NADH and ascorbic acid (AA), the interference between NADH and AA was studied using the N-DNW electrode. Interference by AA is a major problem during the EC determination of biological substrates such as dopamine and NADH.[63,85] To overcome

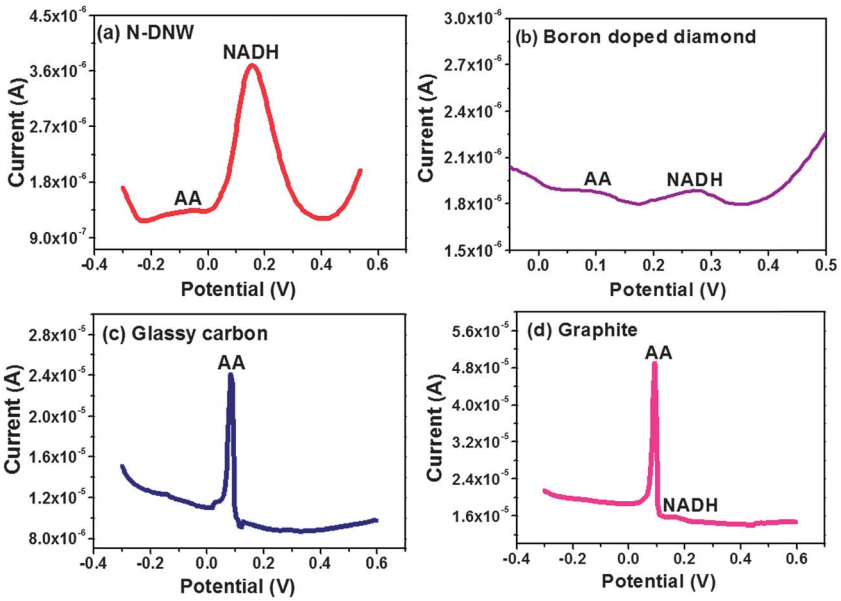

Fig. 3 DPV curves for (a) N-DNW, (b) BDD, (c) glassy carbon and (d) graphite in a solution containing 0.33 mM AA + 0.033 mM NADH. Pulse time = 70 ms, pulse amplitude = 50 mV.

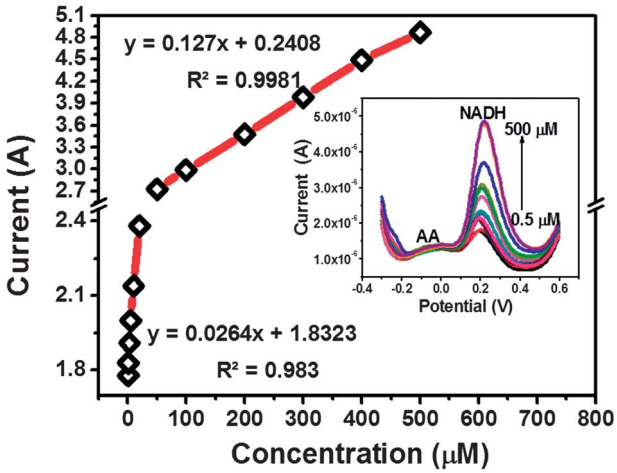

Fig. 4 Calibration plot of N-DNW electrode in 0.1 M PBS (pH 7.4) at different NADH concentrations from 0.5 μM to 500 μM with a constant AA concentration of 0.33 mM. Inset: shows corresponding differential pulse voltammogram. Pulse time = 70 ms, pulse amplitude = 50 mV, interval time = 0.2 s, step potential = 0.5 mV and scan rate = 10 mV s^{-1}.

this problem, the bare electrode surface should be modified carefully with selected mediators, to reduce or prevent the possibility of electrode fouling. Thus, the electrode was modified with Nafion, which electrostatically excluded anions such as ascorbate. However, such membranes usually cause a reduction in the sensitivity. Furthermore, at neutral pH, NADH is negatively charged, and thus it is also excluded by the membrane.[8] Alternatively, ascorbate oxidase, an enzyme, can be used to oxidize ascorbate selectively in the presence of molecular oxygen. Due to the higher sensitivity of pulse techniques, DPV was used to further investigate the ability of the N-DNW electrode to act as a sensor for NADH. Fig. 3 shows the DPV responses of 0.33 mM of AA and 0.033 mM of NADH in pH 7.4 PBS at N-DNW, BDD, graphite, and glassy carbon electrodes. The peak at +0.0 V is due to the electrooxidation of AA along with the NADH signal at +0.15 V, this equates to a peak separation of 150 mV for the N-DNW electrode, which indicates that the N-DNW is highly sensitive towards NADH detection and does not undergo any electrode fouling. Note that the peaks for AA and NADH are not well resolved when the BDD electrode was used this is due to the oxidation of AA at the lower degree of EC reversibility which may lead to the adsorption of ascorbate anion thus hindering the further oxidation of NADH, whereas, glassy carbon and graphite electrodes undergo electrode passivation from the strong adsorption of NAD^+ from the oxidation of NADH. The N-DNW was further used to detect NADH at a wide range of concentrations in the presence of constant AA concentration. As indicated, the anodic peak current increased with increasing NADH concentration, whereas the AA peak current remained constant as is shown in the inset of Fig. 4. The corresponding plots of the currents with respect to the analyte concentrations are plotted in Fig. 4. A linear relationship between the current and the concentration of NADH was obtained for the concentration range of 0.5–10 μM, as shown in Fig. 4. The linear regression equation was I_p (μA) = $0.127_{[NADH]}$ (μM) + 0.2408 μA in the presence of AA, with a correlation coefficient 0.9949, $N = 13$. The detection limit was found to be 0.3 μM and the sensitivity was 26.3 mA M^{-1}. The oxidation current of NADH increased with an increase of NADH concentration. However, when the concentration of NADH was greater than 50 μM, the oxidation current increased slowly. In contrast, the NADH oxidation current was linearly proportional to its concentration in the low concentration range, from 0.5 to 10 μM, as shown in Fig. 4. At the higher concentration range, the solution became saturated and the current response decreased. Thus a change in the calibration slope was observed. The high sensitivity of the N-DNW originates mainly from the very low background current (Fig. not shown), which can be attributed to several factors, including negligible porosity, lack of electroactive carbon-oxygen functional groups and a low density of surface states at the Fermi level compared to that of a metal.[31] The presence of graphitic carbon in the N-DNW film electrode provides strong evidence for the existence of an sp^2 carbon network. Such nanowire like morphology has significant implications for outstanding electrochemical performance in the *in situ* detection of NADH in the presence of AA. The dynamic range, detection limit and lower oxidation potential using a DNW electrode without surface modification are comparable to those of other modified electrodes like BDD, graphite, carbon nanotube, nanocarbon modified GC electrodes found in the literature (Table 1).[86–90]

Table 1 Comparison of N-DNW electrode with previously published other electrode materials for the detection of NADH using CV[a]

Electrodes	Detection range	Oxidation potential	References
DMF-exfoliated graphene	1–360 μM	+0.4 V	81
Bifunctional poly(thionine)-modified electrode	200 μM to 5 mM	+0.2 V	82
Fe_3O_4 nanoparticles/multiwalled carbon nanotubes	1–256 μM	+0.0 V	30
Azine/hydrogel/nanotube composite	0.5–150 μM	+0.1 V	83
Boron-doped carbon nanotubes	0.05 μM to 1 mM	+0.3 V	50
Multiwalled carbon nanotube–alumina-coated silica nanocomposite	5–200 μM	+0.7 V	84
Edge plane pyrolytic graphite electrode	8.2–108 μM	+0.4 V	85
BDD – enzyme immobilised	—	+0.6 V	20
N-DNW (unmodified)	0.5–500 μM	+0.15 V	This work

[a] The detection limit and sensitivity for N-DNW electrode was found to be 0.3 μM and 26.3 mA M^{-1} respectively.

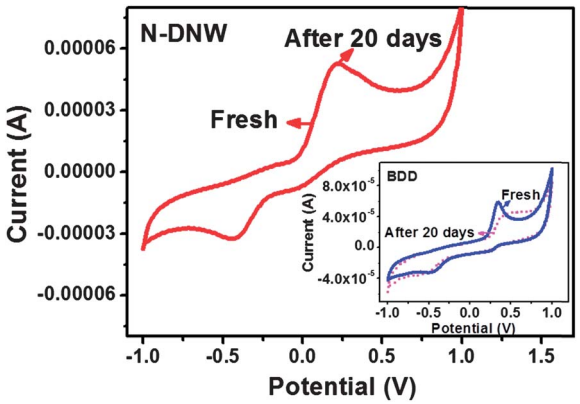

Fig. 5 Cyclic voltammograms for N-DNW and BDD (inset) electrodes were obtained before and after storage in the laboratory for 20 days in 0.1 M PBS (pH 7.4) containing 0.1 mM NADH at a scan rate of 50 mV s^{-1}.

3.4. Stability of the electrode surface during EC oxidation of NADH

Fig. 5a shows the cyclic voltammograms obtained for the oxidation of NADH at a fresh N-DNW electrode and at the same electrode after 20 days of contact with the laboratory air. The oxidation peak potential at the N-DNW electrode remains unchanged even after exposure to the solution, followed by washing, drying, and storage in laboratory air for 20 days. Moreover, the response was found to be stable for several days, even with repeated use. In contrast, for the BDD electrode a positive shift (about 47 mV) in the oxidation peak was observed, demonstrating the rapid deactivation of the electrode (inset of Fig. 5a). This shift was mainly due to the strong adsorption of the NAD^+ produced at the electrode during the oxidation of NADH.[14] Fujishima *et al.* observed that prolonged use (~1 month) of a highly doped BDD electrode resulted in a shift of the oxidation potential up to 80 mV.[1] In addition, unmodified GC electrodes also undergo rapid deactivation during the oxidation of NADH with a more positive anodic shift.[2] The long-term stability of the EC behavior for NADH oxidation on the N-DNW electrode can be attributed to a lack of adsorption on the as-deposited surface.

4. Conclusion

This work demonstrates that the N-DNW electrode can effectively lower the overpotential for the oxidation of NADH. This is believed to be related to the formation of an sp^2 graphitic phase together with diamond. The nanowire-like granular structure helps to enhance the electron transfer behavior. The unmodified N-DNW electrode surface avoids the fouling which commonly hampers carbon based NADH sensors. The combination of long-term stability, high reproducibility and low operating potential of N-DNW films are superior to previous reports. It is noteworthy that these advantages are inherent in the as-made material, and are not the result of surface treatment or modification. The range, sensitivity and detection limit of the N-DNW sensor compare favorably with the values reported for other electrode systems. Selective detection of NADH is also found to be possible in the presence of AA. N-DNW film electrodes show excellent electrocatalytic activity towards the oxidation of NADH in the presence of AA.

Acknowledgements

The authors thank the National Science Council, Taiwan for financial support under the NSC 99-2119-M-032-003-MY2 and NSC 100-2113-M-007-006 contracts.

References

1 T. N. Rao, I. Yagi, T. Miwa, D. A. Tryk and A. Fujishima, *Anal. Chem.*, 1999, **71**, 2506.
2 F. Pariente, F. Tobalina, G. Moreno, L. Hernandez, E. Lorenzo and H. D. Abruna, *Anal. Chem.*, 1997, **69**, 4065.
3 B. Prieto-Simon and E. Fabregas, *Biosens. Bioelectron.*, 2004, **19**, 1131.
4 C. O. Schmakel, K. S. V. Santhanam and P. J. Elving, *J. Am. Chem. Soc.*, 1975, **97**, 5083.
5 J. J. Sun, J. J. Xu, H. Q. Fang and H. Y. Chen, *Bioelectrochem. Bioenerg.*, 1997, **44**, 45.
6 P. N. Barlett, P. R. Birkin and E. N. K. Wallace, *J. Chem. Soc., Faraday Trans.*, 1997, **93**, 1951.
7 Q. Wu, M. Maskus, F. Pariente, F. Tobalina, V. M. Fernandez, E. Lorenzo and H. D. Abruna, *Anal. Chem.*, 1996, **68**, 3688.
8 F. Pariente, E. Lorenzo, F. Tobalina and H. D. Abruña, *Anal. Chem.*, 1995, **67**, 3936.
9 T. Huang, A. Warsinke, T. Kuwana and F. W. Scheller, *Anal. Chem.*, 1998, **70**, 991.
10 W. J. Blaedel and R. A. Jenkins, *Anal. Chem.*, 1975, **47**, 1337.
11 W. M. Clark, *Oxidation Reduction Potentials of Organic Compounds*, The Williams and Wilkins Co., Baltimore, MD, 1960.
12 H. J. Jaegfeldt, *J. Electroanal. Chem.*, 1980, **110**, 295.
13 A. A. Karyakin, E. E. Karyakina, W. Schuhmann and H. L. Schmidt, *Electroanalysis*, 1999, **11**, 553.
14 L. Gorton and E. Dominguez, in *NAD(P)$^+$/NAD(P)H in Living Systems (Encyclopedia of Electrochemistry)*, ed. A. J. Bard and M. Stratmann, Wiley-VCH, Weinheim, 2002, vol. 9, p. 77.
15 A. M. Wilson and D. G. Epple, *Biochemistry*, 1966, **5**, 3170.
16 J. N. Burnett and A. L. Underwood, *Biochemistry*, 1965, **4**, 2060.
17 R. W. Burnett and A. L. Underwood, *Biochemistry*, 1968, **7**, 3328.
18 R. D. Braun, K. S. V. Santhanam and P. J. Elving, *J. Am. Chem. Soc.*, 1975, **97**, 2591.
19 J. Moiroux and P. J. Elving, *J. Electroanal. Chem.*, 1979, **102**, 93.
20 M. A. Hayes and W. G. Kuhr, *Anal. Chem.*, 1999, **71**, 1720.
21 J. Moiroux and P. J. Elving, *Anal. Chem.*, 1979, **51**, 346.
22 J. Moiroux and P. J. Elving, *J. Am. Chem. Soc.*, 1980, **102**, 6533.
23 M. Musameh, J. Wang, A. Merkoci and Y. Lin, *Electrochem. Commun.*, 2002, **4**, 743.

24 C. M. Maroneze, L. T. Arenas, R. C. S. Luz, E. V. Benvenutti, R. Landers and Y. Gushikem, *Electrochim. Acta*, 2008, **53**, 4167.
25 A. S. Santos, A. C. Pereira, N. Duran and L. T. Kubota, *Electrochim. Acta*, 2006, **52**, 215.
26 A. Salimi, S. Lasghari and A. Noorbakhash, *Electroanalysis*, 2010, **22**, 1707.
27 A. Balamurugan and S. M. Chen, *Sens. Actuators, B*, 2008, **129**, 850.
28 L. Meng, P. Wu, G. Chen, C. Cai, Y. Sun and Z. Yuan, *Biosens. Bioelectron.*, 2009, **24**, 1751.
29 K. M. Manesh, P. Santhosh, A. Gopalan and K. P. Lee, *Talanta*, 2008, **75**, 1307.
30 H. Teymourian, A. Salimi and R. Hallaj, *Biosens. Bioelectron.*, 2012, **33**, 60.
31 S. Jolley, M. Koppang, T. Jackson and G. M. Swain, *Anal. Chem.*, 1997, **69**, 4099.
32 J. Xu and G. M. Swain, *Anal. Chem.*, 1998, **70**, 1502.
33 L. F. Li, D. Totir, B. Miller, G. Chottiner, A. Argoitia, J. C. Angus and D. A. Scherson, *J. Am. Chem. Soc.*, 1997, **119**, 7875.
34 T. Yano, D. A. Tryk, K. Hashimoto and A. J. Fujishima, *J. Electrochem. Soc.*, 1998, **145**, 1870.
35 M. Musameh, J. Wang, A. Merkoci and Y. Lin, *Electrochem. Commun.*, 2002, **4**, 743.
36 J. Moiroux and P. J. Elving, *Anal. Chem.*, 1978, **50**, 1056.
37 S. Raina, W. P. Kang and J. L. Davidson, *Diamond Relat. Mater.*, 2008, **17**, 896.
38 J. B. Posthill, D. P. Malta, T. P. Humphreys, G. C. Hudson, R. E. Thomas, R. A. Rudder and R. J. Markunas, *J. Appl. Phys.*, 1996, **79**, 2722.
39 J. Isberg, J. Hammersberg, E. Johnannson, T. Wilkstrom, D. J. Twitchen, A. J. Whitehead, S. E. Coe and G. A. Scarsbrook, *Science*, 2002, **297**, 1670.
40 R. Torz-Piotrowska, A. Wrzyszczyński, K. Paprocki, M. Szreiber, C. Uniszkiewicz and E. Staryga, *J. Achievements Mater. and Manufacturing Eng.*, 2009, **37**, 486.
41 P. Actis, A. Denoyelle, R. Boukherroub and S. Szunerits, *Electrochem. Commun.*, 2008, **10**, 402.
42 B. J. Venton and R. M. Wightman, *Anal. Chem.*, 2003, **75**, 414A.
43 R. M. Wightman, L. J. May and A. C. Michael, *Anal. Chem.*, 1988, **60**, 769A.
44 J. A. Stamfold and J. B. Justice, *Anal. Chem.*, 1996, **68**, 359A.
45 A. Sakharova, L. Nyikos and Y. Pleskov, *Electrochim. Acta*, 1992, **37**, 973.
46 K. Patel, K. Hashimoto and A. Fujishima, *J. Photochem. Photobiol., A*, 1992, **65**, 419.
47 R. Tenne, K. Patel, K. Hashimoto and A. Fujishima, *J. Electroanal. Chem.*, 1993, **347**, 409.
48 G. M. Swain and R. Ramesham, *Anal. Chem.*, 1993, **65**, 345.
49 T. N. Rao and A. Fujishima, *Diamond Relat. Mater.*, 2000, **9**, 384.
50 C. Deng, J. Chen, X. Chen, C. Xiao, Z. Nie and S. Yao, *Electrochem. Commun.*, 2008, **10**, 907.
51 A. Fujishima, T. N. Rao, E. Popa, B. V. Sarada, I. Yagi and D. A. Tryk, *J. Electroanal. Chem.*, 1999, **473**, 179.
52 S. Bhattacharyya, *Phys. Rev. B: Condens. Matter Mater. Phys.*, 2004, **70**.
53 K. J. Sankaran, P. T. Joseph, N. H. Tai and I. N. Lin, *Diamond Relat. Mater.*, 2010, **19**, 927.
54 C. R. Lin, W. H. Liao, D. H. Wei, J. S. Tsai, C. K. Chang and W. C. Fang, *Diamond Relat. Mater.*, 2011, **20**, 380.
55 D. Zhou, A. R. Krauss, L. C. Qin, T. G. McCauley, D. M. Gruen, T. D. Corrigan, R. P. H. Chan and H. Gnaser, *J. Appl. Phys.*, 1997, **82**, 4546.
56 J. Birrell, J. E. Gerbi, O. Auciello, J. M. Gibson, D. M. Gruen and J. A. Carlisle, *J. Appl. Phys.*, 2003, **93**, 5606.
57 Y. C. Chen, N. H. Tai and I. N. Lin, *Diamond Relat. Mater.*, 2008, **17**, 457.
58 J. S. Tsai, C. K. Chang and W. C. Fang, *Diamond Relat. Mater.*, 2011, **20**, 380.
59 R. Arenal, P. Bruno, D. J. Miller, M. Bleuel, J. Lal and D. M. Gruen, *Phys. Rev. B: Condens. Matter Mater. Phys.*, 2007, **75**.
60 A. R. Sobia, S. Adnan, A. Mukhtiar, A. A. Khurram, A. A. Turab, A. Awaisa, A. Naveed, Q. J. Faisal, H. Javaid and G. Yu, *Curr. Appl. Phys.*, 2012, **12**, 712.
61 S. A. Rakha, G. Yu, J. Cao, S. He and X. Zhou, *J. Appl. Phys.*, 2010, **107**, 114324.
62 K. Teii and T. Ikeda, *Diamond Relat. Mater.*, 2007, **16**, 753.
63 K. J. Sankaran, J. Kurian, H. C. Chen, C. L. Dong, C. Y. Lee, N. H. Tai and I. N. Lin, *J. Phys. D: Appl. Phys.*, 2012, **45**, 365303.
64 S. A. Solin and A. K. Ramdas, *Phys. Rev. B: Solid State*, 1970, **1**, 1687.
65 J. W. Ager, D. K. Veirs and G. M. Rosenblatt, *Phys. Rev. B: Condens. Matter*, 1991, **43**, 6491.
66 M. Mermoux, B. Marcus, G. M. Swain and J. E. Butler, *J. Phys. Chem. B*, 2002, **106**, 10816.
67 J. E. Butler and A. V. Sumant, *Chem. Vap. Deposition*, 2008, **14**, 145.
68 J. Birrell, J. E. Gerbi, O. Auciello, J. M. Gibson, J. Johnson and J. A. Carlisle, *Diamond Relat. Mater.*, 2005, **14**, 86.
69 X. Xiao, J. Birrell, J. E. Gerbi, O. Auciello and J. A. Carlisle, *J. Appl. Phys.*, 2004, **96**, 2232.
70 Q. Chen, D. M. Gruen, A. R. Krauss, T. D. Corrigan, M. Witek and G. M. Swain, *J. Electrochem. Soc.*, 2001, **148**, E44.
71 W. A. Yarbrough and R. Messier, *Science*, 1990, **247**, 688.
72 R. J. Nemanich, J. T. Glass, G. Lucovsky and R. E. Shroder, *J. Vac. Sci. Technol., A*, 1988, **6**, 1783.
73 A. C. Ferrari and J. Robertson, *Phys. Rev. B: Condens. Matter*, 2001, **63**.
74 H. Kuzmany, R. Pfeiffer, N. Salk and B. Gunther, *Carbon*, 2004, **42**, 911.
75 Sh. Michaelson and A. Hoffman, *Diamond Relat. Mater.*, 2006, **15**, 486.
76 S. Gupta, B. R. Weiner and G. Morell, *Appl. Phys. Lett.*, 2003, **83**, 491.
77 K. J. Sankaran, K. Panda, B. Sundaravel, H. C. Chen, I. N. Lin, C. Y. Lee and N. H. Tai, *ACS Appl. Mater. Interfaces*, 2012, **4**, 4169.
78 J. Shalini, K. J. Sankaran, C. L. Dong, C. Y. Lee, N. H. Tai and I. N. Lin, *Nanoscale*, 2013, **5**, 1159.

79 J. Shalini, Y. C. Lin, T. H. Chang, K. J. Sankaran, H. C. Chen, I. N. Lin, C. Y. Lee and N. H. Tai, *Electrochim. Acta*, 2013, **92**, 9.
80 B. A. Deore and M. S. Freund, *Chem. Mater.*, 2005, **17**, 2918–2923.
81 J. Chen, J. Bao, C. X. Cai and T. Lu, *Anal. Chim. Acta*, 2004, **516**, 29–34.
82 L. Wu, X. Zhang and H. Ju, *Anal. Chem.*, 2007, **79**, 453–458.
83 E. Katz and I. Willner, *ChemPhysChem*, 2004, **5**, 1084–1104.
84 M. Musameh, J. Wang, A. Merkoci and Y. Lin, *Electrochem. Commun.*, 2002, **4**, 743–746.
85 J. Xu, Q. Chen and G. M. Swain, *Anal. Chem.*, 1998, **70**, 3146.
86 G. P. Keeley, A. O'Neill, M. Holzinger, S. Cosnier, J. N. Coleman and G. S. Duesberg, *Phys. Chem. Chem. Phys.*, 2011, **13**, 7747.
87 S. Baskar, J. L. Chang and J. M. Zen, *Biosens. Bioelectron.*, 2012, **33**, 95.
88 M. T. Meredith, F. Giroud and S. D. Minteer, *Electrochim. Acta*, 2012, **72**, 207.
89 S. J. Wang, H. W. Liaw and Y. C. Tsai, *Electrochem. Commun.*, 2009, **11**, 733.
90 C. E. Banks and R. G. Compton, *Analyst*, 2005, **130**, 1232.